

Terahertz Memos

Memo 05

September 2010

# Optimization of the substrate height for a copper SWO radiator above a copper ground plane

Prashanth Kumar<sup>1</sup>, Carl E. Baum<sup>1</sup>, Kenneth F. McDonald<sup>2</sup>,  
Christos G. Christodoulou<sup>1</sup> and Edl Schamiloglu<sup>1</sup>

<sup>1</sup>University of New Mexico  
Department of Electrical and Computer Engineering  
Albuquerque, NM 87131

<sup>2</sup>Sci-Eng Solutions, LLC  
3304 Lake Town Dr.  
Columbia, MO 65203

## Abstract

This paper explores the quality factor,  $Q$ , resonant frequency,  $f_0$ , and radiated power density,  $P_{\text{rad}}$ , as a function of the height of a (lossless) polyethylene substrate between a copper SWitched Oscillator (SWO) antenna and a copper ground plane. The effects of varying the relative permittivity of the substrate medium are also investigated. Empirical relations for  $Q$  and  $f_0$  as a function of the height and relative permittivity of the substrate medium are obtained using curve fits.

# 1 Introduction

A SWO configuration with a vacuum “substrate” between a copper SWO and a copper ground plane was studied in [1]. The resistive losses as a function of the SWO height,  $h$ , above the ground plane were assessed by examining the quality factor,  $Q$ . We now extend this study to include a substrate medium. We wish to optimize  $h$  to obtain the desired  $Q$  while maximizing the radiated power. This paper explores,  $Q$ , the resonant frequency,  $f_0$ , and the radiated power density,  $P_{\text{rad}}$ , as a function of the height of a (lossless) polyethylene substrate between a copper SWO and a copper ground plane. The effects of varying the relative permittivity of the substrate medium are also investigated.

## 2 Simulation

### 2.1 $Q$ , $f_0$ , and $P_{\text{rad}}$ as a function of $h$

#### 2.1.1 Setup

The setup, probe placements and CST simulation parameters are identical to those in [1] except that a polyethylene substrate,  $\epsilon_{rs} = 2.25$ , is used between the copper SWO and the copper ground plane. Ideally, one desires a substrate with a relative permittivity as close to air as possible, to avoid losses, mostly due to impedance mismatches and surface waves. Polyethylene was chosen as it has a low relative permittivity, is readily available and lends itself easily to fabrication. The substrate is assumed to be lossless. The height of the SWO above the ground plane,  $h$ , is varied.

The dimensions of the SWO, substrate and ground plane are summarized in Table. 1. Note that, due to the substrate medium, the wavelength is reduced as  $\lambda = \lambda_0/\sqrt{\epsilon_{rs}} = (2/3)\lambda_0$ .

Table 1: Dimensions for a copper SWO above a copper ground plane with a (lossless) polyethylene substrate medium.

Parameter	Dimensions ( $\mu\text{m}$ )
Antenna length, $l_a$	$\lambda/2 = 200$
Antenna height (thickness)	1
Switch length, $l_s$	$\lambda/50 = 8$
Antenna width, $w$	$(l_a - l_s)/2 = 96$
Height of substrate, $h$	$\lambda/4 \leq h \leq \lambda/20$
Length of substrate and ground plane	$3\lambda = 1200$
Width of substrate and ground plane	$3\lambda = 1200$
Height of ground plane (thickness)	1

#### 2.1.2 Results

Table. 2 summarizes the peak electric field ( $E_{\text{max}}$ ), resonant frequency ( $f_0$ ) and quality factor ( $Q$ ) as a function of  $h$ . There is little deviation in  $f_0$  compared to that in  $Q$ . The mean  $f_0$  is 0.371

THz with a standard deviation of 0.0074.

Table 2: Variation of the peak electric field ( $E_{\max}$ ), resonant frequency ( $f_0$ ) and quality factor ( $Q$ ) with the height of the SWO above the ground plane ( $h$ ) with a lossless polyethylene substrate.

$h/\lambda$	$E_{\max}$ (V/m)	$f_0$ (THz)	$Q$
0.050	24.508	0.373	49.896
0.075	30.037	0.379	34.519
0.100	33.819	0.38	24.38
0.125	36.116	0.378	18.039
0.150	37.316	0.374	13.815
0.175	37.242	0.37	10.946
0.200	35.846	0.366	8.864
0.225	33.335	0.363	7.31
0.250	30.187	0.359	6.123

The  $Q$ s with and without the substrate, [1], are compared in Fig. 2.1. The results are almost identical. A relation between  $Q$  and  $h/\lambda$  can be obtained by fitting a curve. A function of the form

$$Q(h/\lambda, l_a, \epsilon_{rs}, l_s, w) = a(l_a, \epsilon_{rs}, l_s, w) \left[ \frac{h}{\lambda} \right]^{-n}, \quad 0.05 \leq \frac{h}{\lambda} \leq 0.25, \quad (2.1)$$

is chosen based on analytical expectations. Note that  $Q$  and  $a$  are, in general, also a function of  $l_a$ ,  $\epsilon_{rs}$ ,  $l_s$  and  $w$ . Since  $l_a$ ,  $\epsilon_{rs}$ ,  $l_s$  and  $w$  are fixed, Table. 1,  $Q$  is only a function of  $h/\lambda$  and  $a$  is constant. For the results with the substrate in Fig. 2.1 the fit coefficients are  $a \approx 1.5$  and  $n \approx 1.2$ , i.e.,

$$Q(h/\lambda) \approx \frac{3}{2} \left[ \frac{h}{\lambda} \right]^{-\frac{6}{5}}, \quad 0.05 \leq \frac{h}{\lambda} \leq 0.25, \quad (2.2)$$

For two arbitrary configurations,  $\alpha$  and  $\beta$ , we have

$$\frac{Q_\alpha^n}{Q_\beta^n} = \frac{h_\alpha/\lambda_\alpha}{h_\beta/\lambda_\beta}, \quad (2.3)$$

i.e.,  $h_\alpha/\lambda_\alpha = h_\beta/\lambda_\beta \Rightarrow Q_\alpha = Q_\beta$  regardless of the substrate medium used, which explains the identical results for  $Q$  with and without the substrate in Fig. 2.1. Individual plots for the far-field electric field in the time and frequency domains for each data point, with the substrate medium, in Table 2 are given in the appendix.

To gain more insight into the effect of  $h$  on the radiation characteristics of the antenna, the radiated power densities,  $P_{\text{rad}}$ , at  $r = 1$  m in the  $\theta = 90^\circ$  plane, at the resonant frequencies for various  $h$  are compared in Fig. 2.2. Note that the radiated power is approximately 500% greater for  $\lambda/20$  compared to  $\lambda/4$ . The radiation  $Q$ s and the peak radiated power densities (at  $r = 1$  m) for various  $h$  are compared in Fig. 2.3 which tends to suggest that for maximum radiated power and high  $Q$ , both of which are desired,  $h \lesssim \lambda/10$ .

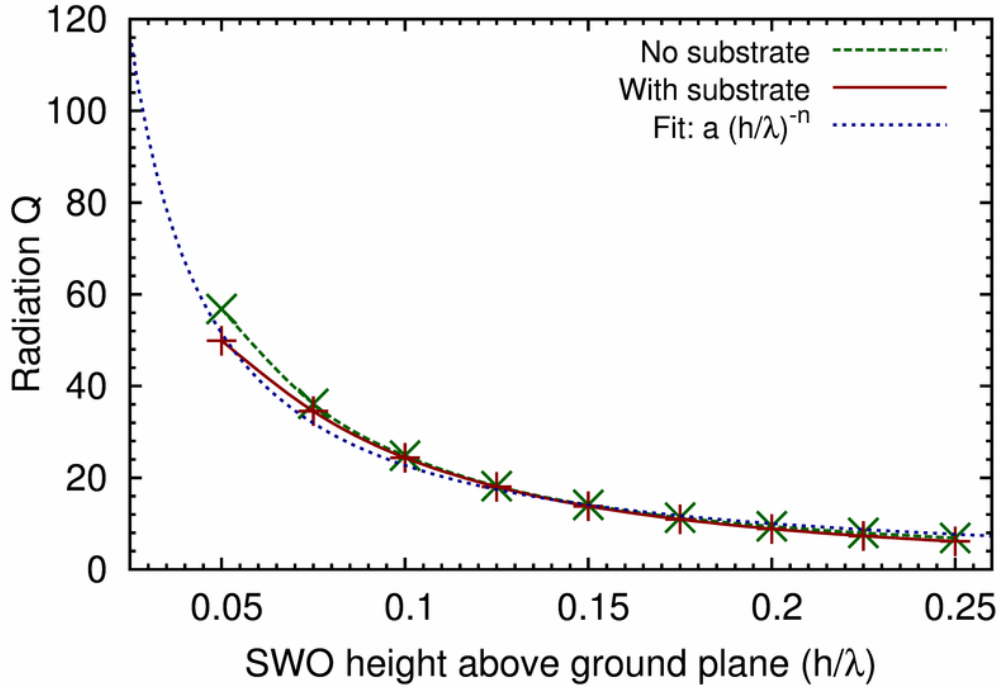


Figure 2.1: Comparison of quality factors ( $Q$ ), as a function of the SWO height above the ground plane, with and without the polyethylene substrate medium. A function is fit to the results, with the substrate, to obtain a more accurate relation between  $Q$  and  $h$ .

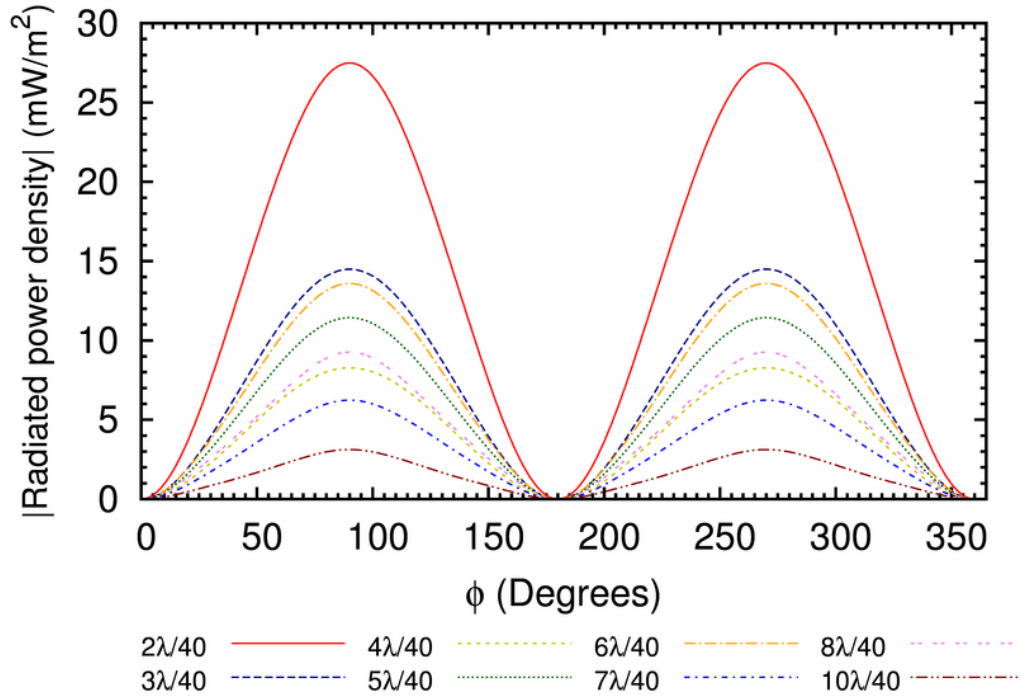


Figure 2.2: Comparison of the radiated power density,  $P_{\text{rad}}$ , at  $r = 1$  m in the  $\theta = 90^\circ$  plane, at the resonant frequencies for various SWO heights above the ground plane.

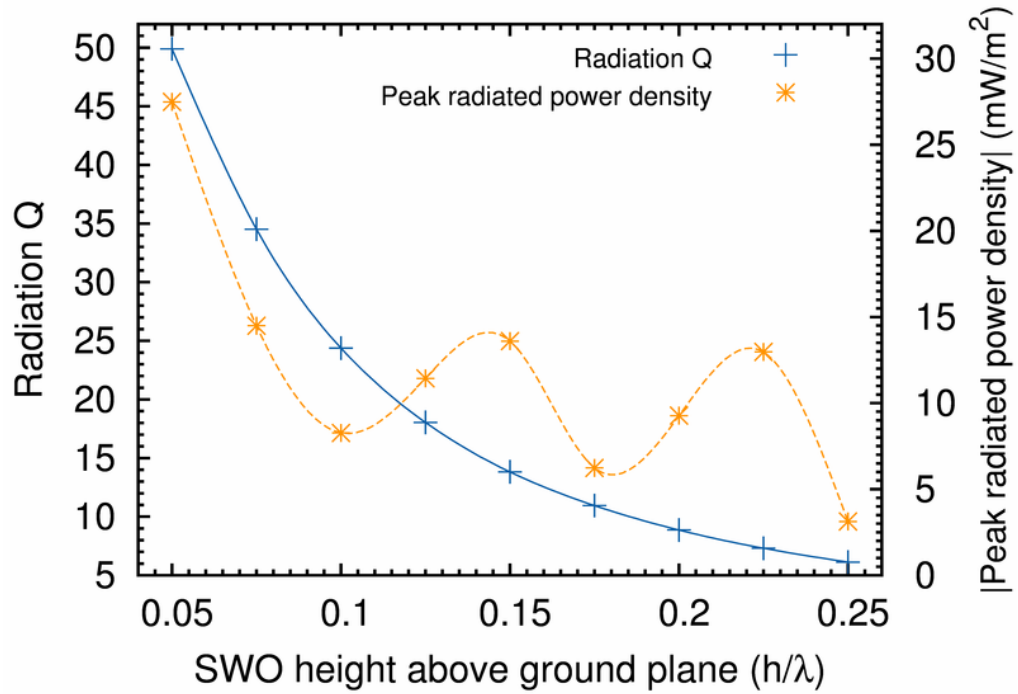


Figure 2.3: Comparison of the quality factor and the peak radiated power density (at  $r = 1$  m) as a function of the SWO height above the ground plane.

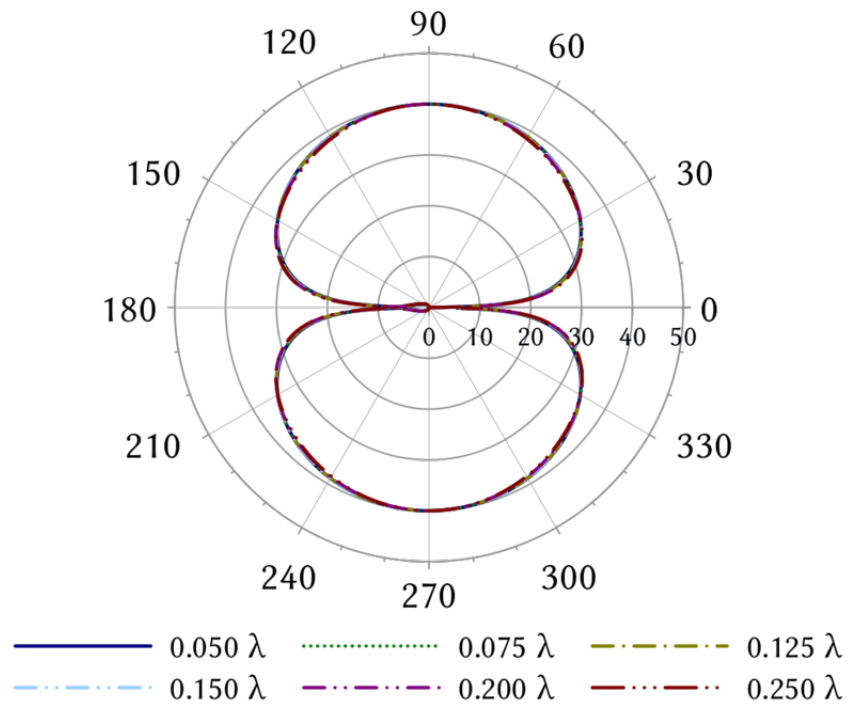


Figure 2.4: Normalized (to 40 dB) polar plot of the radiated power density,  $P_{\text{rad}}$ , (in the  $\theta = 90^\circ$  plane), at the resonant frequencies for various SWO heights above the ground plane, to ascertain the shape of the radiation pattern. The radial scale is 10 dB/div.

The far-field radiated power density patterns, normalized to 40 dB, for various  $h$ , at the respective resonant frequencies, are compared in Fig. 2.4. The radiation patterns are dipolar.

Besides the quality factor and radiated power density, a second constraint on the substrate height is imposed by the *duration* of the radiation,  $\tau$ , i.e., the time taken for the far-field electric field to completely decay to zero. This is dictated by the lifetime of the carriers in the photoconductive region of the switch. For our application, we desire a long carrier lifetime and therefore use SI-GaAs, which has a carrier lifetime in the 50-100 ps range. Examining the far-field electric field pulses in the appendix one notes that the longest time for decay is, for  $h = \lambda/20$ , approximately 120 ps.

## 2.2 $Q$ , $f_0$ , and $P_{\text{rad}}$ as a function of $\epsilon_{\text{rs}}$

### 2.2.1 Setup

The setup, probe placements and CST simulation parameters are identical to those in Sec. 2.1.1 except that the relative permittivity of the substrate medium is varied from  $\epsilon_{\text{rs}} = 2.0$  to  $\epsilon_{\text{rs}} = 10.0$ ; a range of practical interest. The substrate medium is assumed to be lossless for all  $\epsilon_{\text{rs}}$ . The height of the SWO above the ground plane,  $h$ , is fixed relative to each substrate medium at  $h = \lambda/8 = \lambda_0/(8\sqrt{\epsilon_{\text{rs}}})$ .

The dimensions of the SWO, substrate and ground plane are summarized in Table. 3. Since  $\lambda = \lambda_0/\sqrt{\epsilon_{\text{rs}}}$ , the antenna and ground plane dimensions are scaled with respect to each  $\epsilon_{\text{rs}}$ . As in [1],  $\lambda_0 = 600 \mu\text{m}$  corresponding to a frequency of 0.5 THz.

Table 3: Dimensions for a copper SWO above a copper ground plane with a substrate medium of varying relative permittivity ( $\epsilon_{\text{rs}}$ ).

Parameter	Dimensions ( $\mu\text{m}$ )
Antenna length, $l_a$	$\lambda/2$
Antenna height (thickness)	1
Switch length, $l_s$	$\lambda/50$
Antenna width, $w$	$(l_a - l_s)/2$
Height of substrate, $h$	$\lambda/8$
Length of substrate and ground plane	$3\lambda$
Width of substrate and ground plane	$3\lambda$
Height of ground plane (thickness)	1

$\lambda = \lambda_0/\sqrt{\epsilon_{\text{rs}}}$ ;  $\lambda_0 = 600 \mu\text{m}$ ;  $\epsilon_{\text{rs}}$  is varied from 2 to 12.

### 2.2.2 Results

Table. 4 summarizes the peak electric field ( $E_{\text{max}}$ ), resonant frequency ( $f_0$ ) and quality factor ( $Q$ ) as a function of  $\epsilon_{\text{rs}}$ . One observes that  $f_0$  increases with  $\epsilon_{\text{rs}}$  while there is no significant change in the corresponding  $Q$ .

Table 4: Variation of the peak electric field ( $E_{\max}$ ), resonant frequency ( $f_0$ ) and quality factor ( $Q$ ) with the relative permittivity of the substrate medium ( $\epsilon_{\text{rs}}$ ).

$\epsilon_{\text{rs}}$	$E_{\max}$ (V/m)	$f_0$ (THz)	$Q$
2	37.764	0.355	18.121
3	32.269	0.437	17.934
4	28.181	0.506	17.629
5	25.487	0.57	17.083
6	22.68	0.626	16.598
7	20.488	0.677	16.475
8	18.638	0.725	16.181
9	16.981	0.771	15.837
10	15.47	0.813	15.713

Fig. 2.5 shows a plot of  $f_0$  versus  $\epsilon_{\text{rs}}$ . Consider a function of the form

$$f_0(\epsilon_{\text{rs}}, l_a, h, l_s, w) = b(l_a, h, l_s, w)\epsilon_{\text{rs}}^m, \quad 2 \leq \epsilon_{\text{rs}} \leq 10, \quad (2.4)$$

where  $f_0$  and  $b$  are, in general, also a function of  $l_a$ ,  $h$ ,  $l_s$  and  $w$ . Since  $l_a, h, l_s$  and  $w$  are fixed, Table. 3,  $f_0$  is only a function of  $\epsilon_{\text{rs}}$  and  $b$  is constant. For the results in Fig. 2.5, the fit coefficients are  $b = 0.25$  and  $m = 0.52$ . Noting that  $m \approx 0.5$ , one obtains the simple relation

$$f_0(\epsilon_{\text{rs}}) \approx \frac{\sqrt{\epsilon_{\text{rs}}}}{4} \text{ THz}, \quad 2 \leq \epsilon_{\text{rs}} \leq 10, \quad (2.5)$$

As seen in Sec. 2.1.2, where  $\epsilon_{\text{rs}} = 2.25$  was fixed and  $h$  was varied,  $f_0$  is practically independent of  $h$ .

The peak radiated power densities, at  $r = 1$  m in the  $\theta = 90^\circ$  plane, at the resonant frequencies, were found to be relatively constant and less than  $20 \text{ mW/m}^2$  for all  $\epsilon_{\text{rs}}$ . The far-field radiated power density patterns, normalized to 40 dB, for various  $h$ , at the respective resonant frequencies, are compared in Fig. 2.6. Again, one notes that the radiation patterns are dipolar.

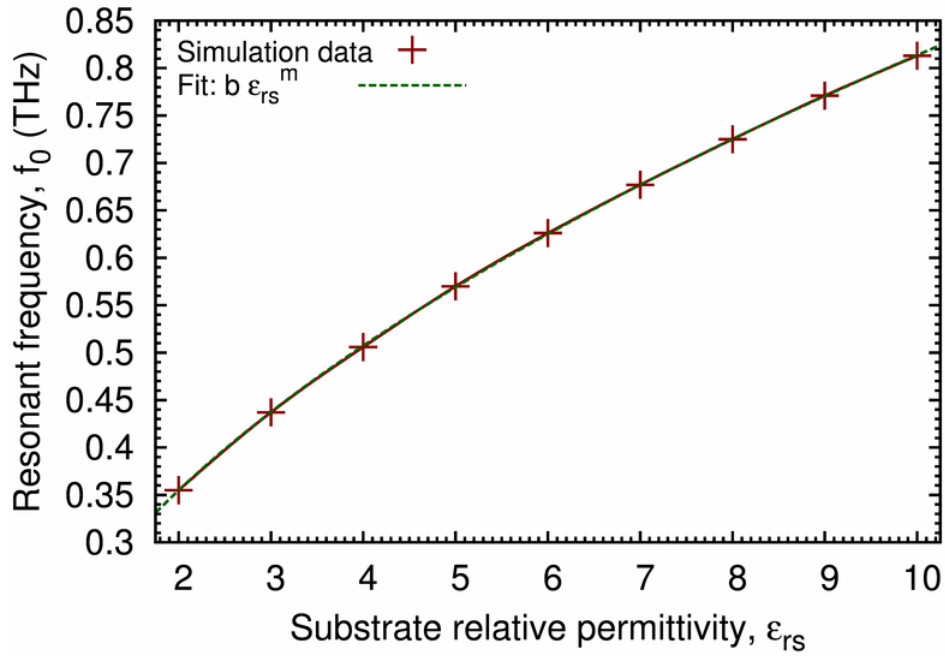


Figure 2.5: The resonant frequency,  $f_0$ , as a function of the relative permittivity of the substrate medium,  $\epsilon_{rs}$ . A function is fit to the results to obtain an empirical relation between  $f_0$  and  $\epsilon_{rs}$ .

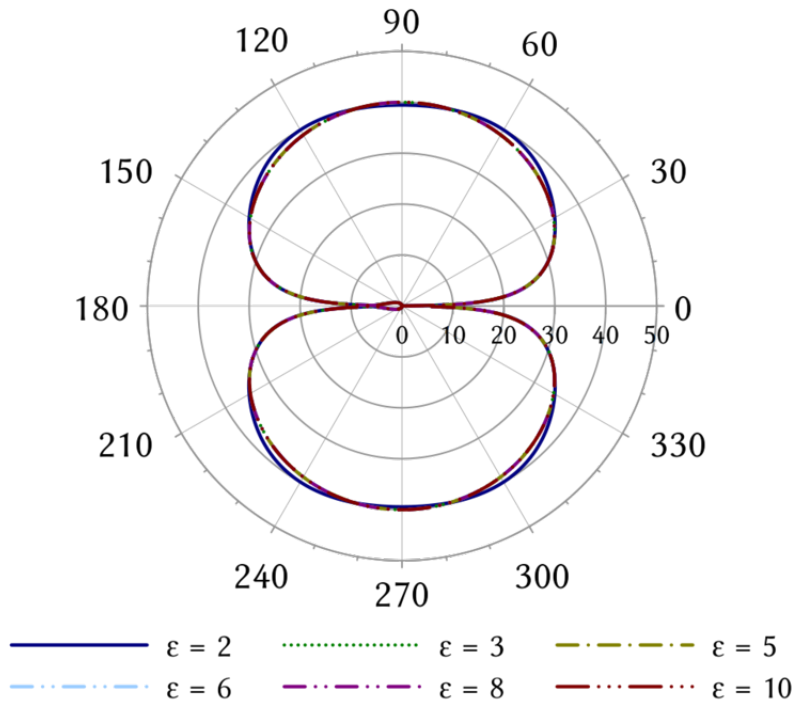


Figure 2.6: Normalized (to 40 dB) polar plot of the radiated power density,  $P_{rad}$ , (in the  $\theta = 90^\circ$  plane), at the resonant frequencies for various  $\epsilon = \epsilon_{rs}$ , to ascertain the shape of the radiation pattern. The radial scale is 10 dB/div.



### 3 Conclusions

- For a large  $Q$  and large radiated power the range of the substrate height is  $\frac{2\lambda}{40} < h \leq \frac{4\lambda}{40}$ .  $Q$  is a function of  $h/\lambda$  while  $f_0$  is practically independent of  $h/\lambda$ .
- The relative permittivity of the substrate medium,  $\epsilon_{rs}$ , only affects the resonant frequency and not the  $Q$ .
- For  $w = \lambda/4$ ,  $l_a = \lambda/2$ ,  $l_s = \lambda/50$  and a lossless substrate medium the following empirical relationships between  $Q$ ,  $h/\lambda$ ,  $f_0$  and  $\epsilon_{rs}$  are obtained,

$$\begin{aligned} - Q(h/\lambda) &= Q(h, \epsilon_{rs}) \approx \frac{3}{2} \left[ \frac{h}{\lambda} \right]^{-\frac{6}{5}} = \frac{3}{2} \left[ \frac{\lambda_0}{h\sqrt{\epsilon_{rs}}} \right]^{\frac{6}{5}}, \quad 0.05 \leq \frac{h}{\lambda} \leq 0.25 \\ - f_0(\epsilon_{rs}) &\approx \frac{\sqrt{\epsilon_{rs}}}{4} \text{ THz}, \quad 2 \leq \epsilon_{rs} \leq 10 \end{aligned}$$

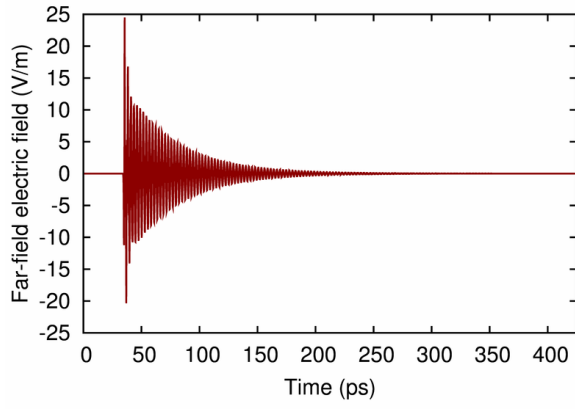
Of course the above results are very specific, since only one parameter is varied at a time while other parameters are held constant. Nevertheless, these results provide valuable insight and can be used to optimize the SWO antenna.

### References

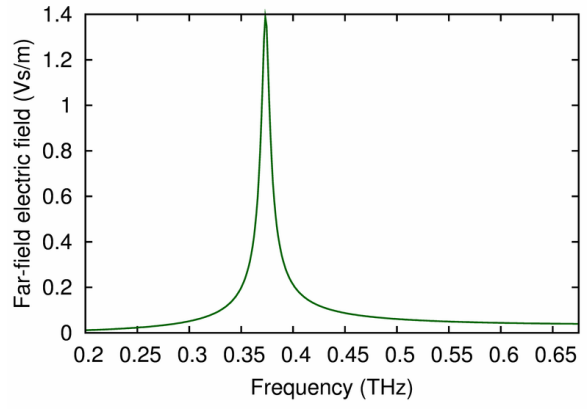
- [1] Prashanth Kumar, Carl E. Baum, Kenneth F. McDonald, Christos G. Christodoulou and Edl Schamiloglu, "Investigation of the skin-effect losses in a copper SWO antenna above a copper ground plane," *Terahertz Memo 4*, Aug. 2010.

# Appendix

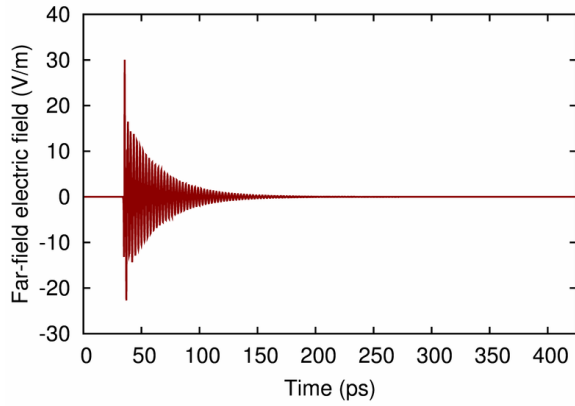
Radiated far-field electric fields, in the time and frequency domains, as a function of  $h$  with a lossless polyethylene substrate medium.



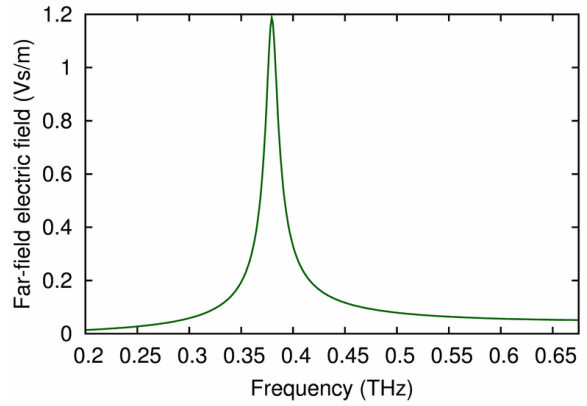
(a)  $h = 0.050\lambda$ .



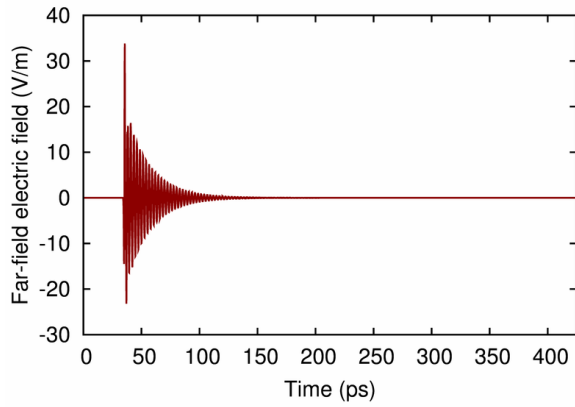
(b)  $h = 0.050\lambda$ .



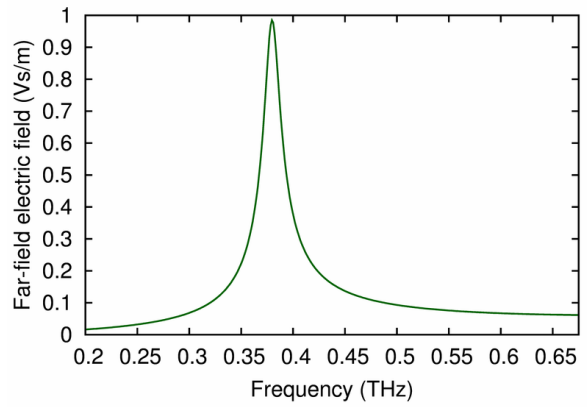
(c)  $h = 0.075\lambda$ .



(d)  $h = 0.075\lambda$ .

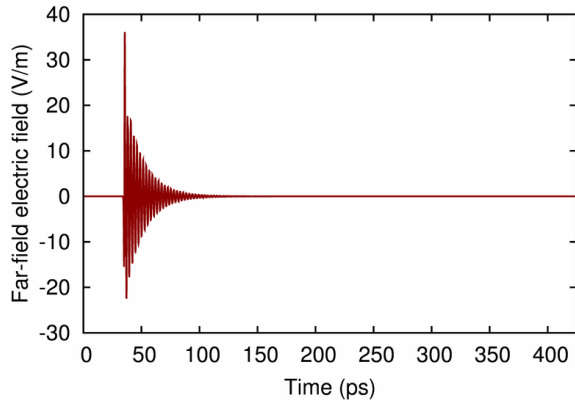


(e)  $h = 0.100\lambda$ .

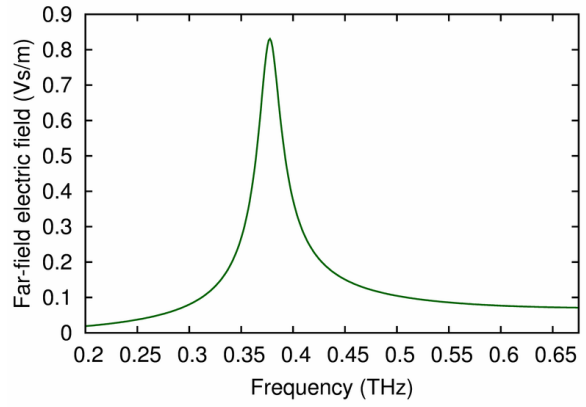


(f)  $h = 0.100\lambda$ .

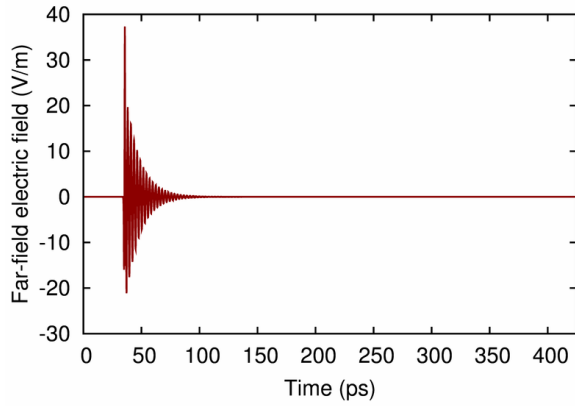
Figure 3.1: Radiated far-field electric field pulse in the time and frequency domains for  $h = 0.50\lambda$ ,  $0.075\lambda$  and  $h = 0.100\lambda$ .



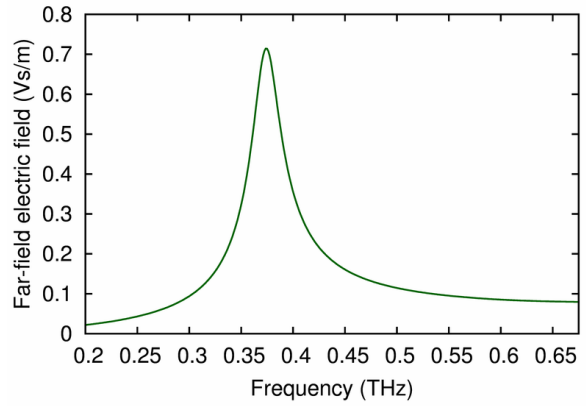
(a)  $h = 0.125\lambda$ .



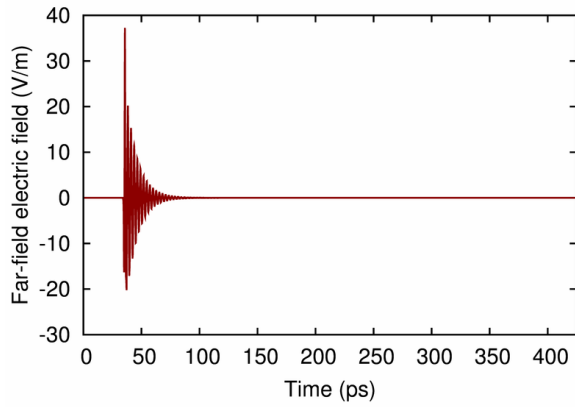
(b)  $h = 0.125\lambda$ .



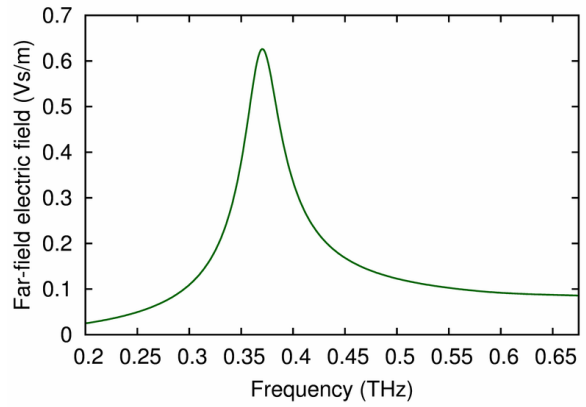
(c)  $h = 0.150\lambda$ .



(d)  $h = 0.150\lambda$ .

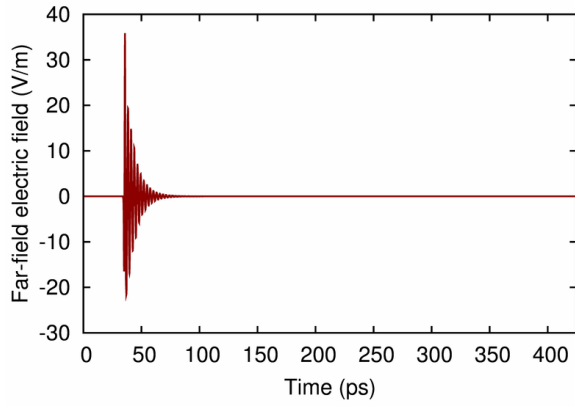


(e)  $h = 0.175\lambda$ .

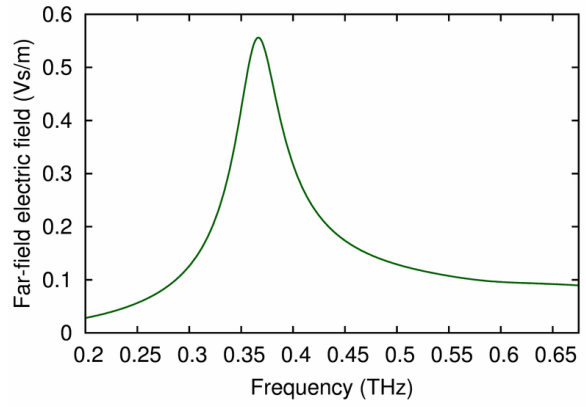


(f)  $h = 0.175\lambda$ .

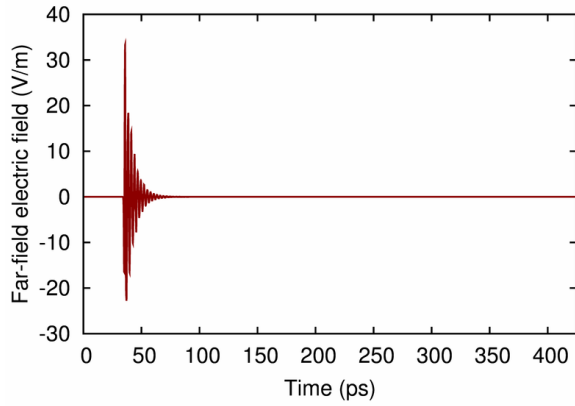
Figure 3.2: Radiated far-field electric field pulse in the time and frequency domains for  $h = 0.125\lambda, 0.150\lambda$  and  $h = 0.175\lambda$ .



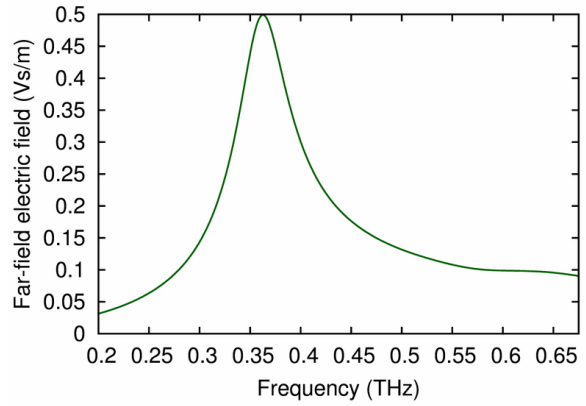
(a)  $h = 0.200\lambda$ .



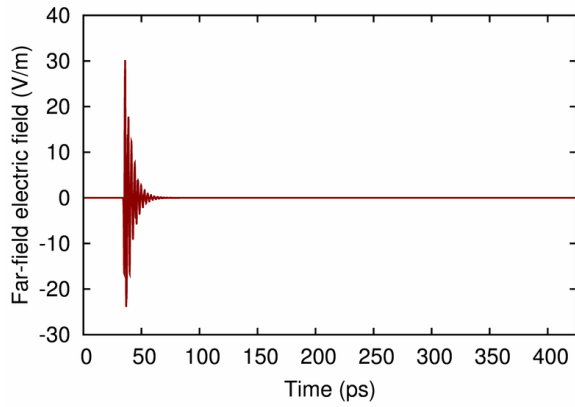
(b)  $h = 0.200\lambda$ .



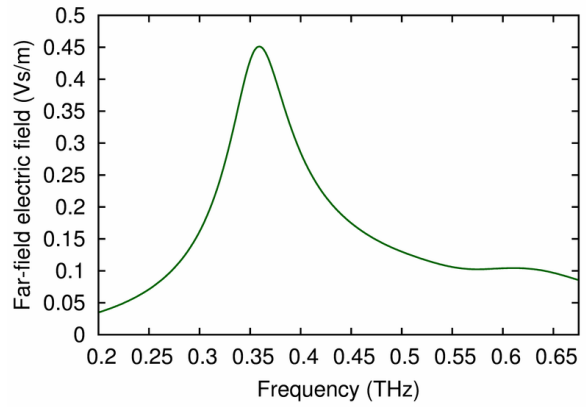
(c)  $h = 0.225\lambda$ .



(d)  $h = 0.225\lambda$ .



(e)  $h = 0.250\lambda$ .



(f)  $h = 0.250\lambda$ .

Figure 3.3: Radiated far-field electric field pulse in the time and frequency domains for  $h = 0.200\lambda, 0.225\lambda$  and  $h = 0.250\lambda$ .